Two-photon fluorescence correlation spectroscopy: FCS

Contact *p.burgos @stfc.ac.uk*

P Burgos

Central Laser Facility, Science & Technology Facilities Council, Rutherford Appleton Laboratory, Harwell Science & Innovation Campus, Didcot, OX11 0QX

Introduction

Fluorescence correlation spectroscopy (FCS) is a powerful single-molecule detection technique used by physicists, chemists, and biologists to characterise the dynamics and interactions of fluorescent species by recording and correlating their fluctuations in fluorescence intensity within a microscopic detection volume[1,2,3]. The spontaneous intensity fluctuations arise from the diffusion (Brownian motion, active transport…) of a few molecules in and out of a restricted sub-micron observation volume defined by a focused laser beam in the sample (~1 fL=10^{-15} L), as well as from any other processes (chemical reactions, photodynamic process, and conformation change) which convert the optical species between states with different emission properties. FCS can provide dynamic information of simultaneous processes occurring on different time scales (from nanosecond to microsecond). In a typical FCS measurement, fluorescence intensity is recorded for a small number of molecules in a specified volume over a time range (generally between 20-60s), and the fluorescence intensity is then analysed in terms of its temporal autocorrelation function G(τ) defined by $G(\tau)=\frac{\langle \delta F(t).\delta F(t+\tau)\rangle}{\langle F\rangle^2}$ (figure 1). The autocorrelation function contains information about equilibrium concentrations, reaction kinetics and diffusion rates of molecules in the sample (2D, 3D, anisotropic diffusion, etc.).

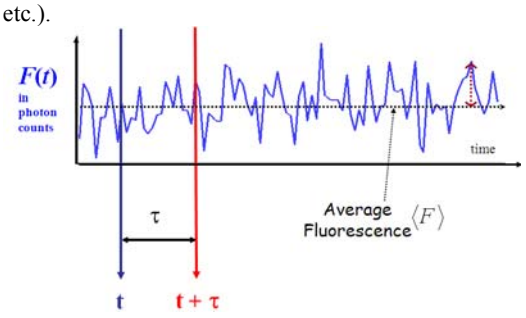

Figure 1: Calculating the autocorrelation function.

Two-photon excitation (TPE), where the fluorophore is excited by simultaneous absorption of two photons, has been applied to FCS for reasons similar to those that have motivated its use in fluorescence microscopy-inherent spatial confinement of excitation, diminished photobleaching and phototoxicity, less scattering, and better optical penetration in turbid media. Moreover it offers the possibility to simultaneously excite several spectrally distinct dyes with a single wavelength for dual-color cross-correlation measurements.

Results

To demonstrate the potential of this technique using our TiSa confocal setup, the diffusion coefficient of the Rhodamine dye was measured for different concentrations and laser powers. Assuming a Gaussian shape for the confocal volume[3], the simplest autocorrelation function for a 3D diffusion is given by:

$$G(\tau)_{3D}=1+\frac{G_{\text{triplet}}(\tau)}{n}\frac{1}{\left(1+\frac{\tau}{\tau_{3D}}\right)\sqrt{\left(1+\frac{\tau}{\tau_{3D}S^2}\right)}} \quad \text{with}$$

$$G(\tau)_{\text{Triplet}}=\left(\frac{1-T+T\cdot\exp(-\tau/\tau_{\text{Tri}})}{1-T}\right)$$

where T denotes the fraction of molecules in the triplet state, τ_{Tri} the triplet lifetime, and n is the number of molecules inside the probed volume. S is the shape parameter of the confocal volume, the ratio between the axial to the radial volume: $S=\frac{\omega_z}{\omega_{xy}}$.

τ_D the diffusion time gives the diffusion coefficient D: $D=\frac{\omega_{xy}^2}{8\tau_D}$ for a two- photon absorption process.

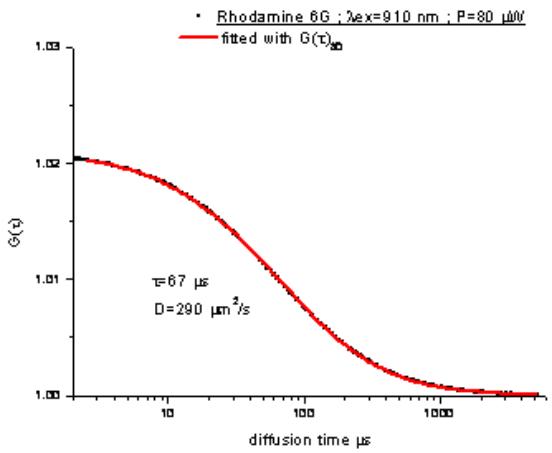

Figure 2: Measuring the diffusion coefficient of Rhodamine 6G in aqueous solution.

The fit (figure 2) gives access to the coefficient of diffusion of the dye (290 $\mu m^2/s$), the concentration of the solution (2.6 nM) and the triplet lifetime (900 ns). The initial amplitude of the autocorrelation function G(τ=0) varies with the inverse of the number of molecules inside the detection volume: the concentration of the solution can be probed (figure 3).

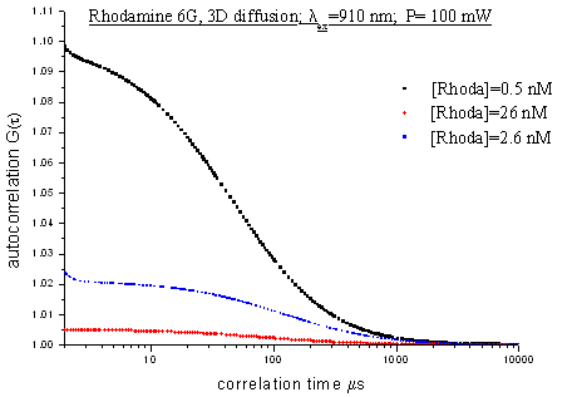

Figure 3: The effect of the particles concentration on the autocorrelation function.

If the laser is too powerful, erronous values for the initial concentration (photobleaching of the dye) and for the diffusion time may result (figure 4).

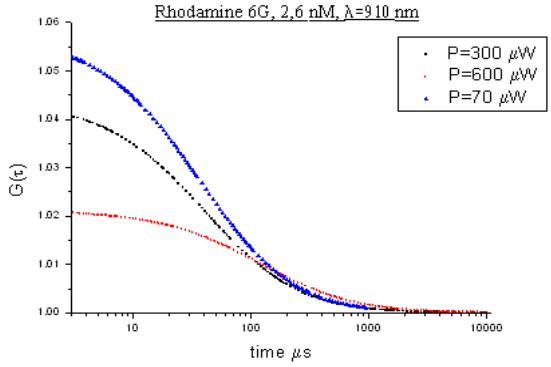

Figure 4: The effect of the laser power on the autocorrelation function.

In figure 5, FCS has been used to measure the mobility of poxvirus inside a live cell using a 2D diffusion model for the data fitting (surface diffusion):

$$G(\tau)_{2D} = 1 + \frac{G_{\text{triplet}}(\tau)}{n} \frac{1}{\left(1 + \frac{\tau}{\tau_{2D}}\right)}$$

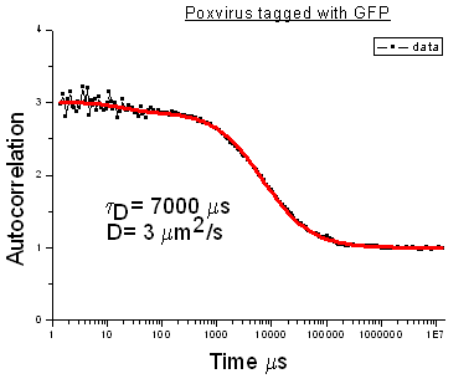

Figure 5: Diffusion of poxvirus inside cell.

With our setup, we can use cross correlation to remove detector noise (after pulse signal), or to probe interactions between two different fluorescent labels with distinct excitation and emission properties.

Conclusion

Fluorescence correlation spectroscopy (FCS) is a technique used for spatial and temporal analysis of molecular interactions in solution (in vitro and in vivo). The power of FCS lies in its capability to extract dynamics (molecular diffusion, dimerization, complex formation, triplet lifetime…) over a wide range of time scales from sample concentrations ranging from subnanomolar to micromolar. Renewed interest in FCS in recent years has been stimulated by the fact that it is inherently miniaturised and therefore applicable for high-throughput screening applications[4].

References

[1] Magde, D., Elson, E. L., Webb, W. W. Thermodynamic fluctuations in a reacting system: Measurement by fluorescence correlation spectroscopy, 1972, *Phys Rev Lett*, **29**, 705–708.

[2] Elson, E. L., Magde, D. Fluorescence correlation spectroscopy I. Conceptual basis and theory, 1974, *Biopolymers*, **13**, 1–27.

[3] Magde, D. Elson, E. L., Webb, W. W. Fluorescence correlation spectroscopy II. An experimental realization, 1974, *Biopolymers*, **13**, 29–61.

[4] Berland, K. M., Fluorescence correlation spectroscopy: a new tool for quantification of molecular interactions, 2004, *Methods Mol Biol*., **261**, 383-394.

The ULTRA time-resolved IR, 2D-IR and T-2D-IR station

Contact *ian.p.clark @stfc.ac.uk*

I P Clark, G M Greetham, P Burgos, P Matousek, A W Parker, M R Pollard, D A Robinson, M Towrie

Science & Technology Facilities Council
Central Laser Facility, Science & Technology Facilities Council, Rutherford Appleton Laboratory, Harwell Science & Innovation Campus, Didcot, OX11 0QX

P S Codd, R C Farrow, M Kogimtzis, Z J Xin

Science & Technology Facilities Council
Technology Department, Science & Technology Facilities Council, Daresbury Laboratory, DSIC, Warrington, Cheshire, WA4 4AD

Q. Cao, M. W. George

University of Nottingham
School of Chemistry, University of Nottingham, University Park, Nottingham, NG7 2RD

Introduction

Ultrafast time-resolved pump-probe spectroscopies are now widely applied techniques for the detection of short-lived reactive intermediates and excited states and provide valuable information on structure and dynamics of molecular species in the condensed phase.[1,2,3]

Over the last three years the LSF has developed the ULTRA facility, the successor to the PIRATE[4]/Kerr-gated Raman[5] system, which along with transient absorption and femtosecond stimulated Raman spectroscopies is optimized for time-resolved infrared investigations of biological species. The system is highly sensitive being capable of measuring changes in sample absorbance of ΔOD *ca* 10^{-5} in 1 second. Along with the high sensitivity the instrument is also extremely flexible for multiple beam experiments such as ground state and transient two-dimensional infrared spectroscopic measurements.

Instrumentation

The system is a custom designed 10 kHz dual titanium sapphire amplifier (Thales Laser) with single oscillator seed source (FemtoLaser). One amplifier produces 40-80 fs pulses while the other produces 1-3 ps pulses both at 10 kHz, 0.8 mJ and 800 nm. The two are synchronized to < 70 fs through the sharing of a single seed source; long term drifts in the timing of the two amplifiers, on the picoseconds timescale, are controlled using feedback to the picosecond regenerative amplifier cavity which contains a piezo stepper motor. This feedback control is vital for transient-2DIR data acquisition where the timing of the fs UV pump and IR probe and ps IR pump must all be kept to sub-ps accuracy.

At their outputs each amplifier is split into two to pump computer-controlled OPAs (TOPAS, Light Conversion) equipped with harmonic units, and sum frequency and difference frequency units. This combination allows wavelengths in the range 200 – 15000 nm to be accessed with either fs or ps pulse lengths. The polarization of all the output beams can be set using either computer-controlled zero order or broadband wave plates. The combination of fs and ps pulse lengths and wide tuning range provides enormous scope for a range of pump-probe techniques including time-resolved infrared (TRIR) spectroscopy and ground state and time-resolved double-resonance two-dimensional IR spectroscopy (2D-IR and T-2D-IR). All these studies employ the fs IR beam, which has a bandwidth of *ca* 500 cm^{-1}, as the probe and use either the fs UV-vis, and/or the ps IR beam with its narrow, 12 cm^{-1}, bandwidth as the pump.

A pump-probe time-delay is introduced and controlled using an optical delay line (Newport), and the pump beam repetition rate reduced using optical choppers (TTi). The repetition rate of the pump is technique dependent, for TRIR and 2D-IR 5 kHz is used and for T-2D-IR 5 kHz and 2.5 kHz are used for the UV and IR pumps respectively. The pump and probe beams are then focused into a temperature-controlled (-60 to > 80 °C) sample cell (Harrick Scientific, 6 µm to 1 mm pathlength) with typical beam diameters of *ca* 100 and 50 µm respectively. To reduce photo-degradation samples are either rastered in the *x,y* plane or rastered and flowed with a minimum flow volume of *ca* 300 µl. The probe beam is then split into two with each half focused into separate spectrographs (0.25 m f/4 DK240, Spectral Products). Light is then detected using 128 element mercury cadmium telluride (MCT) arrays (IR Associates) which are read out by a custom DAQ system (QD).

The spectral window is controlled along with the resolution by using different diffraction gratings and use of the detectors which can either be used as 128 element probe and 128 element reference or 240-250 element (allowing for some spectral overlap) probe by combining the two arrays with the spectrographs tuned to different wavelength regions. The dual-detector approach produces an unsurpassed spectroscopic window of *ca* 500 cm^{-1}. The major influence in background variation in the difference spectra is due to spectral fluctuations which lead to either baseline slope or offset changes. When dual probe detectors are used a 64 element MCT array (Infrared Associates) is used as the reference and is spectrally matched using a combination of interpolation and lower density grating. This referencing allows spectral changes of the order of ΔOD *ca* 10^{-5} in 1 second to be recorded.

The first element of one of the MCT probe detectors is reserved for monitoring IR pump intensities, throughout a 2D-IR spectrum scan, providing the relative pulse intensity data.

The whole of the IR spectroscopy system is purged by nitrogen gas to remove interference from atmospheric water vapour and carbon dioxide which have large absorptions in the *ca* 1600 cm^{-1} and 2400 cm^{-1} regions.

The data acquisition and system is controlled through a NI *LabView* program written in-house. This also controls the scanning of the IR pump beam for the 2D-IR and T-2D-IR experiments and the tuning of the probe OPA. Further details on this can be found in another article in this annual report.

Further information on the instrumentation can be found in reference [6].

Results

To demonstrate the broad bandwidth of the instrument the TRIR spectrum of 4-phenylbenzophenone in CD_3OD was recorded, Figure 1, as a comparison to previously recorded data.[7] The spectrum, which was recorded with a 5 pixel overlap between the two probe detectors, clearly shows the > 500 cm^{-1} bandwidth - ca 4 times that available on the previous PIRATE system.[4]

The negative peaks in the TRIR spectrum of 4-phenylbenzophenone correspond to the loss of the ground

state parent species upon excitation and the positive peaks to the new species formed. In this case two species are produced the singlet excited state, which has peaks at *ca* 1460 and 1554 cm^{-1}, and the ππ* triplet excited state which is responsible for the remaining 7 features. Figure 2 shows the kinetics of the decay of the singlet state leading to the formation of the triplet state which has a rise time of *ca* 15 ps.

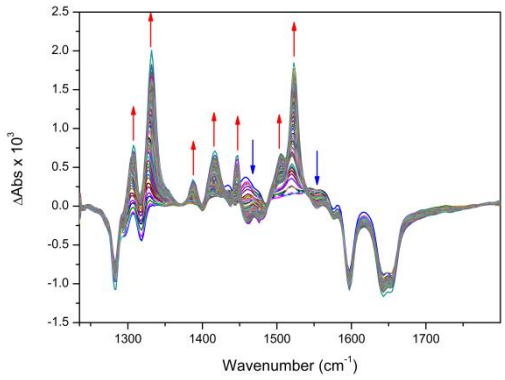

Figure 1 TRIR spectra of 4-phenylbenzophenone in CD_3OD obtained at 1 to 800 ps following irradiation (267 nm, 3 µJ, magic angle polarization) and 100 s data acquisition. Blue arrows mark the decay of the singlet excited state while the red arrows mark the formation of the triplet state.

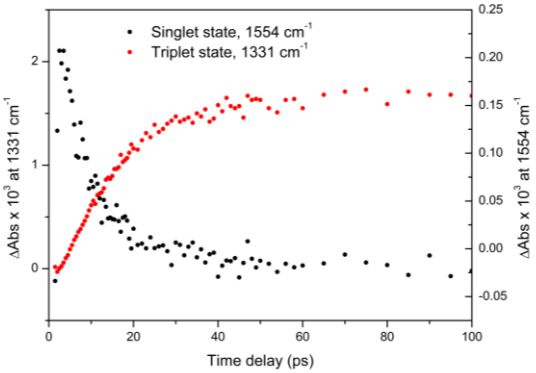

Figure 2 Kinetics of the decay of the singlet excited state of 4-phenylbenzophenone in CH_3OD at 1554 cm^{-1} (filled circles) and rise of the triplet state at 1331 cm^{-1} (open circles).

Figure 3 illustrates the 2D-IR technique, using 5'-GMP in D_2O buffer as an example; for reviews of the technique see references 8 and 9. Here the 1D-IR spectrum lies along the pump-probe frequency diagonal, peaks **1** and **2** are assigned to the carbonyl stretch at 1662 cm^{-1} and ring mode at 1585 cm^{-1} respectively. The main features of interest in 2D-IR spectroscopy are the features that lie off this diagonal, **3**, where pumping of one band at *eg* 1662 cm^{-1} has a significant effect on other vibrations through vibrational coupling. The bleaches (in blue) correspond to loss of the v = 0-1 mode on excitation and the transient absorptions (in red) are those of the v = 1-2 species formed. Spectra recorded at each individual pump wavelength show a slice through the 2D spectrum and the 2D plot is composed of all slices.

An example of the T-2D-IR spectroscopy can be found elsewhere in this report in the article by Dr Neil Hunt.

Conclusions

We have demonstrated the potential of the ULTRA infrared station which can be applied to a wide range of techniques – TRIR, 2D-IR and T-2D-IR, examples of which can be found elsewhere within this report. The instrument is a significant improvement over the PIRATE facility having *ca* 4 times the bandwidth (*ca* 500 cm^{-1}) enabling spectra to be recorded over a wide spectral window in shorter time and with reduced sample quantities, a feature that is particularly important when studying valuable biomolecules. The instrument is aided by advanced control software enabling scanning of the 2D-IR pump wavelengths, delay lines and waveplates permitting many experimental variations to be recorded in a single data file.

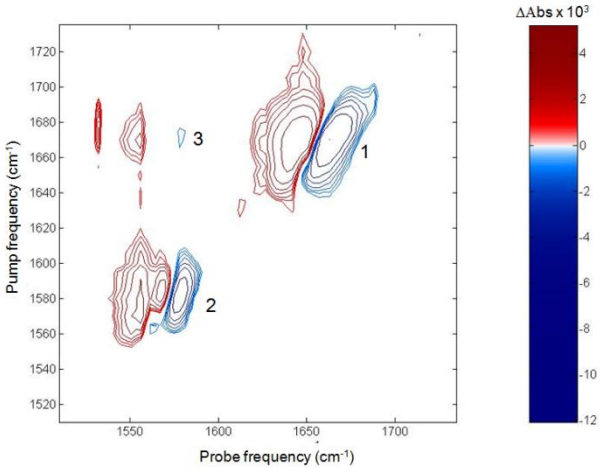

Figure 3 2D-IR spectrum of 5'-GMP (10 mM) in D_2O buffered solution (50 mM phosphate buffer) recorded 2 ps after excitation (*ca* 1 µJ, magic angle polarization).

Acknowledgements

We thank BBSRC and STFC for joint funding of the STFC Facility Grant (ST/501784).

References

[1] Rafal Kania, Andrew I Stewart, Ian P Clark, Gregory M Greetham, Anthony W Parker, Michael Towrie, and Neil T Hunt, Physical Chemistry Chemical Physics : PCCP **12**, 1051-63 (2010).

[2] Michael D Fayer, David E Moilanen, Daryl Wong, Daniel E Rosenfeld, Emily E Fenn, and Sungnam Park, Accounts Of Chemical Research **42**, 1210-1219 (2009).

[3] Luuk J G W van Wilderen, Ian P Clark, Michael Towrie, and Jasper J van Thor, The Journal Of Physical Chemistry B 091201110959003 (2009).

[4] M Towrie, D C Grills, J Dyer, J A Weinstein, P Matousek, R Barton, P D Bailey, N Subramaniam, W M Kwok, C Ma, D Phillips, A W Parker, and M W George, Applied Spectroscopy **57**, 367-80 (2003).

[5] A W Parker, P Matousek, M Towrie, C Ma, W M Kwok, D Phillips, and W T Toner, Journal Of Raman Spectroscopy **32**, 983-988 (2001).

[6] G M Greetham, P Burgos, Q Cao, I P Clark, P S Codd, R C Farrow, M W George, M Kogimtzis, P Matousek, A W Parker, M R Pollard, D A Robinson, Z J Xin, and M Towrie, Submitted.

[7] M W George, C Kato, and H Hamaguchi, Chemistry Letters **22**, 873-876 (1993).

[8] Sang-Hee Shim, David B. Strasfeld, Yun L. Ling, and Martin T. Zanni, Proceedings Of The National Academy Of Sciences Of The United States Of America **104**, 14197-202 (2007).

[9] Neil T Hunt, Chemical Society Reviews **38**, 1837-48 (2009).

Developments within the EPSRC Laser Loan Pool

Contact *ian.p.clark@stfc.ac.uk*

I P Clark, M Towrie, A W Parker

Central Laser Facility
Science & Technology Facilities Council, Rutherford Appleton Laboratory, Harwell Science & Innovation Campus, Didcot, OX11 0QX

Introduction

Throughout 2009/10 the Laser Loan Pool continued to provide laser systems to the UK research community providing a cost effective, valuable resource aiding many research groups and helping in the training of a number of postgraduate students.

Research projects undertaken with the help of the Loan Pool range from magneto-optical data storage to polymer dynamics.

Developments

During the year a number of changes have occurred, the most significant of which is the establishing of a Steering Committee for the facility. This committee consists of four UK researchers with differing areas of expertise, spanning the fields of chemistry, physics, bioscience and materials/engineering research. The committee members are:

- Prof Lin Li – University of Manchester
- Prof Pavlos Lagoudakis
- Dr Andrew Hudson – University of Leicester
- Dr Michael Hippler – University of Sheffield

Members of CLF staff and the Loan Pool steering committee at the January meeting. From left to right, Tony Parker, Pavlos Lagoudakis, Lin Li, Andrew Hudson, Michael Hippler, Mike Towrie and Ian Clark

The first committee meeting was held in January 2010 and was highly productive with a number of key points raised. Research fields that could be better supported by the facility were identified, namely materials and bioscience; in addition the possibility of supplying whole experimental set-ups, for *eg* spectroscopic techniques, was considered but at present is unlikely.

The potential benefits to the community of a wide range of new laser systems were discussed and a number of possible purchases identified. These include a supercontinuum source with acousto-optic tunable filter (AOTF), a femtosecond tunable titanium:sapphire (Ti:S) oscillator with optical parametric oscillator (OPO) and a picosecond high power laser for cold ablation type machining.

Tunable Ti:S oscillator and OPO

A tender exercise is currently in progress for the purchase of this system. The emphasis for this system is ease of use *ie* turn-key, hands-free and computer controlled. This system is expected to appeal to researchers in the fields of physics and bioscience and is designed with coupling into a microscope in mind. Applications are likely to include coherent anti-Stokes Raman spectroscopy (due to the tunable oscillator and OPO), multi-photon excitation microscopy and materials processing. This system is hoped to be in place by December 2010.

Supercontinuum source with AOTF

This laser system with increase the scope of the Loan Pool further having a wide range of potential applications to support research in the fields of physics, chemistry and the life-science interface *eg* single molecule spectroscopy and optical coherence tomography.

This laser has been purchased and is a quasi CW single-mode supercontinuum white light laser from NKT coupled with acousto-optic tunable filter; specifications are provided in the table below. Delivery is expected in early August 2010.

Source	**SuperK G2 Extreme**
Tunability	460-2400 nm
Total average power	> 2 W
Spectral density	2.4 mW/nm max, 0.8 mW/nm min 465-750 nm 2.0 mW/nm max, 0.3 mw/nm min 750-1100 nm 1.2 mW/nm max, 0.3 mW/nm min 1100-2000 nm
Repetition rate	40 MHz
Master source pulse length	5 ps
Polarization	Unpolarized
Ancillaries	SpectraK dual AOTF with single visible AOTF (450-750 nm) and second channel for direct infrared output. Armoured fiber & collimator

In addition to the above specifications the system has a modification in the form of a second amplifier module to permit access to *ca* 100 mW of spectrally clean 1064 nm.

High power laser

This laser would be for the materials and engineering community. However when the necessary ancillary items are taken into account this would be a very costly system and as yet a definite decision on the purchase remains to be made. The Loan Pool would very much welcome the thoughts of the community as to whether this system is desired.

Conclusions

Two new laser systems are to be introduced to the facility by year end with a third under consideration. As such some lasers will be retiring, these will be the current CWL1 argon-ion laser and one of the Nd:YAG pumped dye systems (NSL5), a call for applications for these systems will go out in late summer 2010.

Acknowledgements

The authors gratefully acknowledge the support of the Laser Loan Pool Steering Committee.

The OCTOPUS Imaging Cluster: A New Imaging Facility in the Research Complex at Harwell

S.W. Botchway, D.T. Clarke, M. Hirsch, A. Mackenzie, M.L. Martin-Fernandez, S.R. Needham, S.K. Roberts, D.J. Rolfe, A. Tylee, C.J. Tynan, and S.E.D. Webb

Central Laser Facility, STFC, Rutherford Appleton Laboratory, Research Complex at Harwell, Didcot, Oxon OX11 0FA, UK

Main contact email address: *marisa.martin-fernandez@stfc.ac.uk*

Introduction

The past year has again seen major changes in the Lasers for Science Facility (LSF). The LSF's operations in the biological imaging area were relocated to the Research Complex at Harwell (RCaH) in April 2010. The OCTOPUS (Optics Combined to OutPut Unique Solutions) cluster is a large scale imaging facility offered by the Functional Biosystems Imaging Group (FBI) of the LSF, which begun user operations and collaborative work in July 2010. OCTOPUS is a new concept in multi-modal imaging. Currently in Phase I of its development, the OCTOPUS cluster has at its core a hub of 14 lasers (3 Ti:Sa, 2 OPOs, 3 supercontinuum and 6 CW) (**Fig. 1,2**).

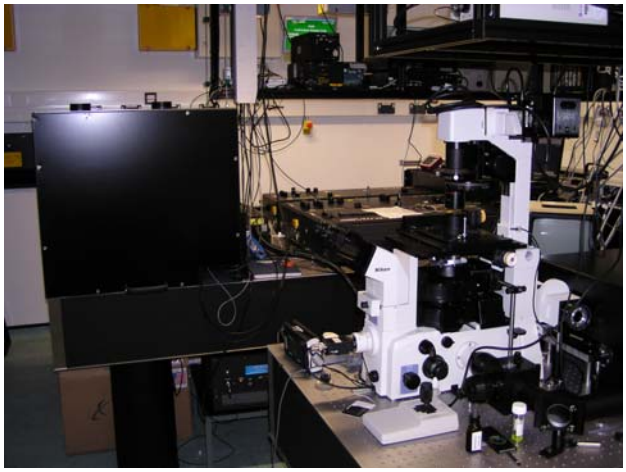

Figure 1. *The laser hub.* *Left: The large black box holds the CW lasers and launchers (See **Fig. 2**). Right: the two Ti:Sa lasers (femtosecond and picoseconds pulses) and an OPO. Bottom right: The two-photon confocal microscope housed in the laser hub.*

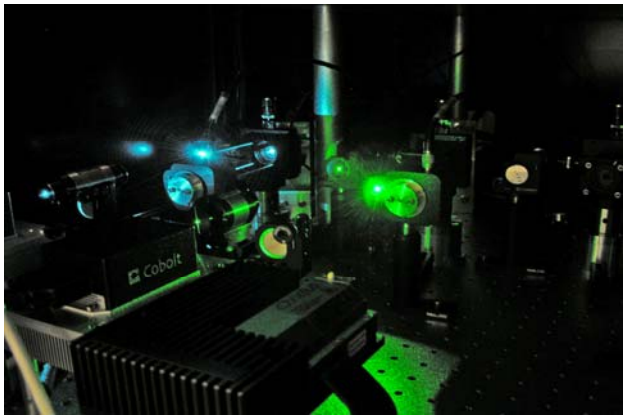

Figure 2. Two *CW lasers launched inside the black box on the left of **Fig. 1** above.*

The laser sources provide excitation light to seven microscope systems, namely a total internal reflection fluorescence (TIRF) tweezers system, 3 single molecule fluorescence microscopes, each specialising in a different single molecule imaging technique, two 1-photon confocal FLIM systems and a 2-photon confocal FLIM system laid out as shown in **Fig.3**.

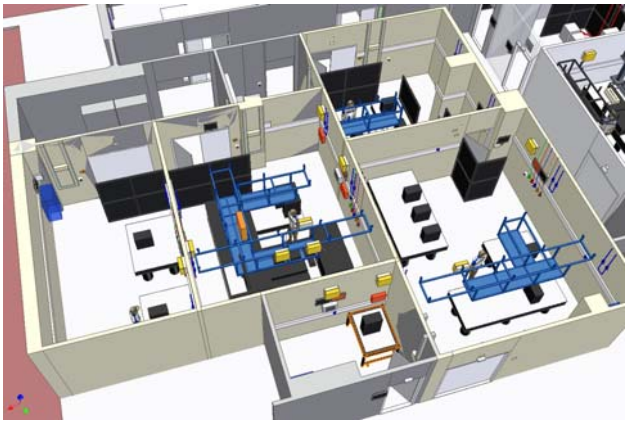

Figure 3. *Layout of the OCTOPUS cluster. The central room is the laser hub with the different microscopes lab position around it. It also houses a two-photon confocal FLIM system. Bottom right: this room houses three systems, namely a TIRF-tweezers system, a one-photon confocal FLIM system and a 5-colour single molecule tracking system. Top right: This room houses a one-photon multicolour confocal FLIM system. Top middle: The control room (see **Fig. 2**). Top left: Storage room. Left: This room houses a 3-colour single molecule tracking system (top) and an 8-channel single molecule FRET and polarisation combined system (bottom). Bottom middle: Development room.*

Figure 4. *OCTOPUS laser control room. For more information contact Andrew.Tylee@stfc.ac.uk.*

In Octopus different laser lines from the central core can be combined to supply 'engineered' illumination (i.e. with different wavelengths and different pulse repetition and length) which is tailor-made to the needs of the experiment. This is achieved through a combination of single mode optical fibres, fibre combiners, the AOTF's outputs from the supercontinuum laser sources and the outputs from the Ti:Sa and OPO sources. The fibres transporting light into the microscopes are interlocked through a central control room that keeps track of which laser is used in which microscope and ensure safe operation (**Fig. 4**). The first generation of OCTOPUS offers the following microscopy stations:

2 colour, 2 polarisation 8-channel single molecule TIRF microscopy. This is a home-built objective-type TIRF microscope illuminated via a single-mode fibre (**Fig. 5**). The excitation polarisation is purified using a Glan-Taylor polariser and then rotated between orthogonal polarisations using an achromatic liquid crystal polarisation rotator. The fluorescence is split into orthogonal emission polarisations in each of two wavelength bands, giving four channels which are imaged onto the CCD simultaneously for each of the two possible excitation wavelengths. Polarisation-sensitive dichroic mirrors are used to ensure that the fluorescence polarisation is not affected. The switching of the rotator is synchronized to acquire images such that alternate frames in a series have the same excitation polarisation. The combination of two colours and two polarisations allows us to monitor the distances between single molecules using Fluorescence Resonance Energy Transfer (FRET), as well as the orientation of the molecules using single molecule polarisation measurements. The microscope uses TIRF illumination, which restricts fluorescence excitation to a layer a few hundred nm thick to reduce the level of out of focus background fluorescence and to allow single molecules to be detected. Quad-View optics split the fluorescence into four spatially identical images on the CCD. The microscope can be used to image single fluorescent molecules in live cells, allowing the monitoring of molecular interactions in real time.

Figure 5. *Left: Experimental setup for 3-colour single molecule tracking system. Right: experimental setup for multidimensional single molecule fluorescence imaging. The picture shows a wall-mounted black panel between the microscopes below the open yellow box on the wall. This black box houses the array of fibre connectors that allow laser light to be transported via fibres, combiners etc. from the adjacent laser hub in the OCTOPUS core to the microscope room through the wall. These boxes can be found in all the labs. A fibre connector and cable is shown hanging below the black box.*

3-colour and 5-colour single molecule TIRF microscope. This microscope is similar to the instrument described above, but allows the imaging of three different fluorophores simultaneously (**Fig. 3**). Multicolour microscopes are required for the investigation of macromolecular interactions in complex networks, for example signalling pathways. A five colour microscope is currently under commissioning (**Fig. 4**) (funded through a BBSRC Long and Large grant awarded jointly to STFC and King's College London).

Confocal Microscopy. OCTOPUS offers three confocal microscopy systems. The Multiphoton FLIM imaging capability located within the laser hub allows the imaging of molecules deep inside living cells (**Fig. 1**). This system is used in several collaborative programmes involving STFC and a number of universities.

Figure 6. *Left hand side: one-photon confocal FLIM system. Right hand side: 5-colour single molecule fluorescence microscope.*

A one-photon confocal FLIM system is currently under commissioning using a newly purchased Becker and Hickl scanning head (**Fig. 6**).

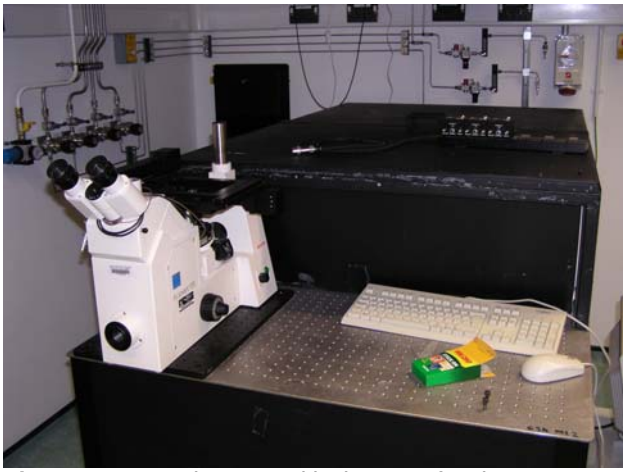

Figure 7. *One-photon multicolour confocal system. In-house built confocal microscope that uses a Fianium supercontinum as laser input.*

OCTOPUS also has a multicolour confocal microscope used to characterise in situ the 3-D structural disposition of macro-molecular complexes at the plasma membrane of cells (**Fig. 7**). Both one-photon confocal FLIM systems have recently been upgraded with the addition of supercontinuum laser sources, which offers almost

limitless flexibility in the choice of fluorescent probes that can be used. Fluorescence correlation imaging has recently been commissioned on this microscope.

TIRF-Tweezers. The TIRF Tweezers setup is designed to combine the optical manipulation of samples with super high-resolution real-time TIRF imaging. A 1064nm laser is propagated through an AOD to enable a fully steerable trap which is focused onto the imaging plane. A Nikon TIRF cassette enables easy manipulation of a fibre laser beam past the critical angle of total internal reflection. The fluorescence emitted is imaged through a Nikon TE-2000 microscope onto a back illuminated Andor EMCCD camera. This will enable real time manipulation and force analysis of structures in biological specimens with minimal cell damage. There is capacity to upgrade the system to incorporate a super-continuum fibre input for multiple excitation and splitting optics for multiple-colour imaging as used in the systems above.

Figure 8. *Left: TIRF-Tweezers set up. Right: One-photon confocal.*

Phase I of the OCTOPUS cluster is now operational in the RCaH. The new location has allowed the integration of all the microscopy stations and laser sources, offering a fully flexible, large scale imaging facility to the user community.

Image Analysis. The analysis of data from single molecule measurements, particularly in live cells, is challenging because the images often have high backgrounds, signals are weak, and the molecules are mobile. The FBI Group has an active programme of development in advanced image analysis methods, using Bayesian techniques. This programme has been funded through a series of research council grants and the software is made available for use by the user community as it is developed.

The Future

Additional microscopy stations will be added as techniques and technology develop, and as the requirements of the community evolve. The location of the Molecular Structural Dynamics arm of the new LSF within RCaH will also allow the formation of an imaging "supercluster", in which large scale pulsed laser systems will be used to image specific molecules in cells without the requirement for labelling.

OCTOPUS will also interact with other facilities on the campus, particularly Diamond Light Source and the proposed Imaging Solutions Centre. Proposed programmes include, for example, the combination of fluorescence, electron, and x-ray microscopy on the same sample, supported by information from macromolecular crystallography and molecular dynamics simulations. This powerful combination, unique to the Harwell campus, will allow us to obtain a complete picture of how the structure of biological macromolecules enables them to fulfil their specific roles in the complex systems that are responsible for the functioning of cells and organisms in health and disease.

References

1. S. E. D. Webb, S. R. Needham, S. K. Roberts, and M. L. Martin-Fernandez. "Multidimensional single-molecule imaging in live cells using total-internal-reflection fluorescence microscopy". Optics Letters, **31**, 2157 (2006).
2. S. E. D. Webb, D. J. Rolfe, S. R. Needham, S. K. Roberts, D. T. Clarke, C. I. McLachlan, M. P. Hobson, M. L. Martin-Fernandez. "Simultaneous widefield single molecule orientation and FRET microscopy in cells". Optics express **16**, 20258 (2008).
3. M. K. Kuimova, S. W. Botchway, A. W. Parker, M. Balaz, H. A. Collins, H. L. Anderson, K. Suhling and P. R. Ogilby. "Imaging intracellular viscosity of a single cell during photoinduced cell death". Nature Chemistry **1**, 69 (2009).

New data analysis software for time-resolved spectroscopy experiments in the ULTRA laser facility

Contact *mark.pollard @stfc.ac.uk*

M R Pollard, G M Greetham, D A Robinson, M Towrie, I P Clark and A W Parker

Science & Technology Facilities Council, Central Laser Facility, Rutherford Appleton Laboratory, Harwell Science and Innovation Campus, Oxfordshire OX11 0QX

Introduction

The ULTRA laser facility is a highly sensitive, time resolved spectrometer that provides valuable information on the structure and dynamics of molecules in solution. A diverse range of spectroscopy experiments can be performed within the ULTRA facility through its synchronised, dual (ps and fs) 10 kHz repetition rate output, with a broad range of wavelength tuning (from UV to mid infrared) [1].

ULTRA produces experimental data through the detection of spectral changes of laser light after transmission through a sample (see Figure 1). Scientists need to analyse this large collection of spectra within minutes to decide if their experiment is following their predictions or whether a modification to the experimental strategy is needed. The need for quick data analysis is vital in experiments where samples have a limited lifetime, potentially being light or temperature sensitive.

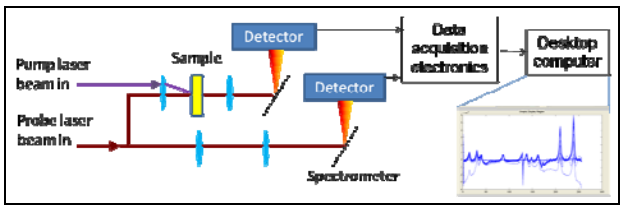

Figure 1 showing overview of typical ULTRA experiment for measurement of laser light absorption by sample. Note the use of two detectors, one immediately after the sample and the other as a reference for later data analysis.

The flexibility of the ULTRA facility introduces a number of variables that must be corrected for in order for meaningful data to be produced, such as variability in laser intensity between pulses, background intensity signals and electronic noise within detectors. The data analysis software was developed to remove these variations and is intended for use throughout the experiment at the Central Laser Facility and as 'take-away' software in the scientists' home institutions.

Software considerations

Previous data analysis performed using Excel spreadsheets was found to be time-consuming and laborious, especially with the increased number of variables and large volumes of data produced within the ULTRA laser facility. The new software automates this preliminary analysis process and presents the original and processed data in order to verify results, in order to confirm that the analysis has not introduced spurious effects in the data.

A set of functions were prioritised for development, principally to display spectral data and correct for instrument variation. The software was built in three stages (data collection and sorting, preconditioning and data display) and assumed the name 'Legobrick' software. A range of software tools were considered (including Labview, C++ and Matlab) and it was decided that Matlab offered the necessary range of functions (for data display, analysis and spreadsheet-like operations) and was familiar to the software developers (D. A. Robinson and M. R. Pollard). The software produces output files in the comma separated variable format (csv), a popular format that allows data to be accessed by other software such as Excel, Origin and Igor during development.

Data collection and sorting

This first elementary step requires the user to identify and load the data files containing spectral data. In the software, the data is assembled as an array, with axes attributed to experimental parameters (e.g. pump – probe pulse delay, polarisation, wavelength etc.).

Preconditioning

The second step removed the variation in data due to instrumentation effects and is shown in Figure 2. The preconditioning window displayed the experimental parameters in a spreadsheet-style data table with plots showing corrected data in two and three dimensions. Instructions for use of the software are given in the caption corner (bottom left in Figure 2).

The various functions corrected effects introduced by the apparatus or elements within the experiment. The instrument effects were corrected using two functions:

- Automatic identification and removal of values from data caused by 'dead' detector pixels.
- Overlap correction, where the spectrum is dispersed over multiple detectors for improved resolution and final spectrum is assembled from multiple detector data sets.

The following experimental effects were corrected:

- Separation of steady state and transient data, using the 'T0 Correction' function to select a value from the data table that represented the steady state background spectrum.
- Subtraction of reference spectral data with 'Reference processing', using data from a second detector (see Figure 1) that measures the intensity and spectral fluctuations of the laser.
- Correction for large scale difference spectra intensity variations using 'Baseline correction function'. This fitted a polynomial to user-defined points in the spectrum and subtracted the baseline from the dataset.

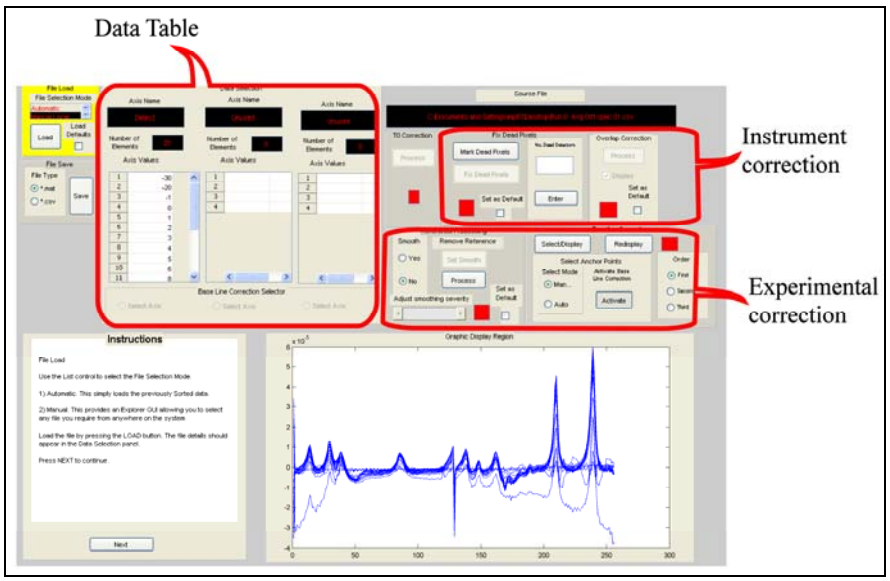

Figure 2 Screenshot of preconditioning window, with functions for data table, instrument and experimental correction highlighted in red

Graphics display

The final part of the software in this report allowed multiple spectra to be compared as one experimental parameter was changed. The graphics display window (see Figure 3) displays two and three dimensional plots of the spectral data, where a dimension refers to the experimental parameter. The parameters were displayed again in a data table format, which allowed users to plot data corresponding to an individual value or a combination of values, for example transient analysis of particular wavelengths or pixels (known as 'kinetics plotting'). The variation of the whole data set could be visualised using the 3d plotting function. A function called 'Release graph' allowed separate figures to be produced for use in journal publications.

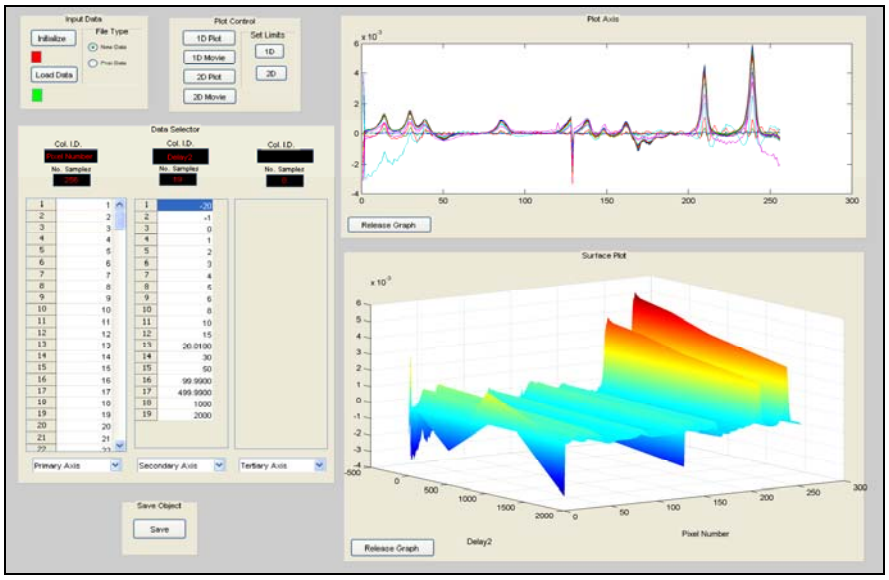

Figure 3 Screenshot of graphics display, showing data from sample of DMABN.

Conclusions

- The finished software is now in use in the ULTRA facility, with a typical day of analysis involving 15 experimental data sets, each consisting > 20 spectra. This permits scientists to efficiently make preliminary analyses and to inform the on-going experimental strategy.
- The data analysis software has been well received by the user community and is used on site and in users' home institutions on a variety of desktop computers and laptops.
- Future versions of the software will allow for different experimental data sets to be imported for comparison and provide a calibration of the spectra relative to wavenumber.

Acknowledgments

We wish to thank D. A. Robinson for his efforts on this valuable work, despite a long period of serious ill health.

References

[1] "Ultra laser system: a new dual-output 10 kHz Ti:Sapphire amplifier with UV–IR generation for time-resolved spectroscopy", G. M. Greetham, P. Matousek, D. A. Robinson, A. W. Parker, M. Towrie, R. C. Farrow, P. S. Codd, Z. J. Xin and M. W. George, CLF Annual Report, (2007-2008).

Active synchronisation of dual amplifier outputs for time-resolved spectroscopy.

Contact *mark.pollard @stfc.ac.uk*

M R Pollard, G M Greetham and M Towrie

Science & Technology Facilities Council, Central Laser Facility, Rutherford Appleton Laboratory, Harwell Science and Innovation Campus, Oxfordshire OX11 0QX

Introduction

The ULTRA laser provides unique capabilities for advanced time-resolved spectroscopy techniques (such as Two-dimensional IR[1] and Femtosecond Stimulated Raman Spectroscopy[2]) that use the combination of dual 2 ps and 50 fs output pulses. The fs and ps amplifiers are synchronised naturally due to their common seed source but thermal drift can occur in the optical paths through the amplifiers and may result in relative timing drifts of several ps at the sample to be studied. Loss of synchronisation at the ps level can significantly affect measurements and so must be corrected. We report a control system that measures the relative timing between the ps and fs pulses and controls their synchronisation to a programmable fs value.

Relative timing measurement

The relative timing measurement takes a ~ 1 % split of the 800 nm light produced from each of the two amplifier stages and cross-correlates the signals to extract timing differences.

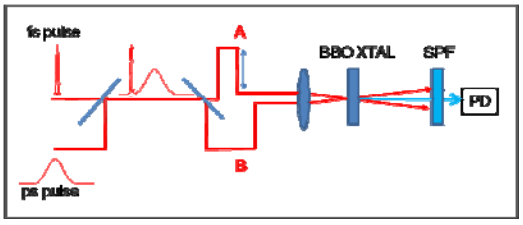

Figure 1. Optical apparatus for relative timing measurement between the ps and fs pulses.

The timing measurement apparatus (shown in Figure 1) combines the ps and fs pulses with a timing difference of ~ 10 ps. The combined pulses pass through a scanning cross-correlator consisting of two beam paths, A and B, with a variable delay on A. The pulses are recombined within a 1 mm BBO crystal (BBO XTAL), where up-conversion to 400 nm occurs when the pulses are overlapped in time. The up-converted signal is filtered by a short pass filter (SPF) and detected by a GaP photodiode (PD) whose output is sampled using a data acquisistion card (National Instruments). The variable delay scans the relative timing of the pulses to produce cross- and auto-correlation peaks, as shown in Figure 2.

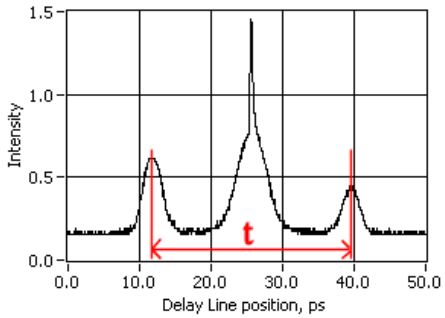

Figure 2. Waveform occurring from the correlation of ps and fs pulses in time.

The correlation waveform in Figure 2 shows three distinct peaks. The centre peak represents the combination of two auto-correlation signals and has a ~ 4 ps broad peak (mixing of ps pulse of arm A with ps pulse of arm B) with a narrow < 100 fs spike (mixing of the fs pulse of arm A with the fs pulse of arm B) at its maximum. The outer peaks in Figure 2 are ~ 2 ps broad and arise from cross-correlation of the ps pulse on one path with the fs pulse on the other path. For example, the ps pulse of arm A of the correlator (Figure 1) mixes with the fs pulse on arm B. The separation between these two cross-correlation peaks (shown as 't' in Figure 2) is equal to twice the relative timing separation between the ps and fs input pulses. The information from the waveform was processed using peak fitting and statistical functions written in Labview software.

Control system

A feedback loop (shown in Figure 3) was used to observe the relative timing measurement and correct any deviation from a defined set-point by adjusting the timing of the ps output pulses, with all functions performed in Labview software.

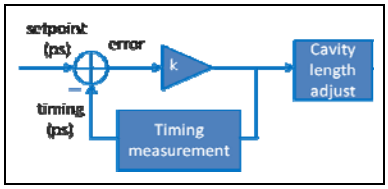

Figure 3 Diagram of control system using a feedback loop.

The timing of the ps output pulses was modified by adjusting the cavity length of the ps regenerative amplifier, by movement of one end mirror on a piezoelectric translation stage, with the magnitude of the adjustment controlled by the proportional gain value k (see figure 3).

Results

The relative timing measurement was performed over 2 hours and was found to drift by 1.5 ps. The control system was activated with a k value of 0.4 and controlled the relative timing to 42 fs rms, with a response time of 1 s, see Figure 4.

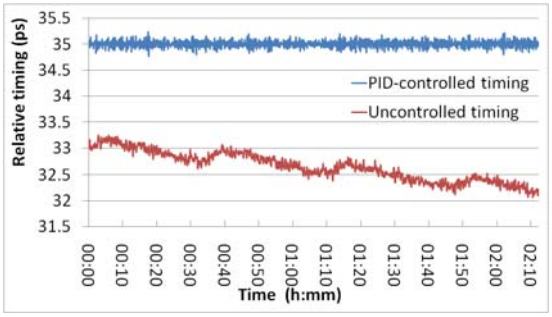

Figure 4 Comparison of relative timing over 2 hours.

References

1. R. Kania, A. I. Stewart, I. P. Clark, G. M. Greetham, A. W. Parker, M. Towrie and N. T. Hunt, Phys. Chem. Chem. Phys. **12** 1051 (2010).
2. Femtosecond stimulated Raman scattering, G. M. Greetham et al, CLF Annual report, pp 182 - 184 2006-7.

Optical trapping of laser targets under vacuum for ion-beam production in the LIBRA programme

Contact *andy.ward@stfc.ac.uk*

A D Ward
Lasers for Science Facility
STFC

B Li
Central Laser Facility
STFC

T Strange
Central Laser Facility
STFC

Introduction

The studies detailed here form part of the EPSRC Basic Technology programme (EP/E035728/1) entitled Laser Induced Beams of Radiation and their Applications (LIBRA). The concept of LIBRA is to develop a new generation of laser-driven ion-beam sources by using a high power laser beam to irradiate small plastic or liquid targets at high repetition rates. The laser's energy causes intense high-energy ionising radiation to be ejected from the surface (Figure 1). The ion-beam technology has the potential for wide ranging applications from cancer treatment and forensics to critical fault diagnosis and three dimensional chemical and structural analysis.

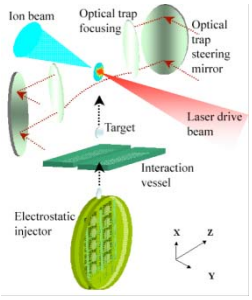

Figure 1: Original design concept for target delivery, optical trapping and target irradiation to produce ion-beams

LIBRA requires technological developments regarding targets, delivery systems, interaction environments, and detectors. The targetry and delivery requirements are foremost in this report as we intend to deliver targets to an interaction area under vacuum and suspend them without physical means of attachment. Physical supports and tethers are known to perturb the ion-beam production mechanism[1] and to generate unnecessary debris. We report the use of laser-based optical levitation and manipulation methods to achieve this goal.

Our aim is to levitate micron-scale targets, under vacuum, using photonic forces and to position the targets with micron accuracy into the beam path of a high power laser for ion-beam production. Here we demonstrate the underpinning methodology and optical requirements for trapping micron-sized droplets at low pressures in a vacuum chamber environment.

Laser Trapping Configuration

Two co-axially aligned, counter-propagating, laser beams (1064 nm) were used to create an optical trap through a balance of opposed scattering forces (Figure 2). Long-working distance objective lenses (working distance 10 mm) with high numerical aperture (NA = 0.7) were used to provide a robust and stable trapping environment for micron-scale targets. The working distance is sufficient to enable debris shielding and propagation of ion-beams without interference from the optical components. The concept of counter propagation has been widely used in literature[2,3,4] to trap aerosol droplets and we would like to develop this methodology further to enable its implementation inside a target interaction chamber.

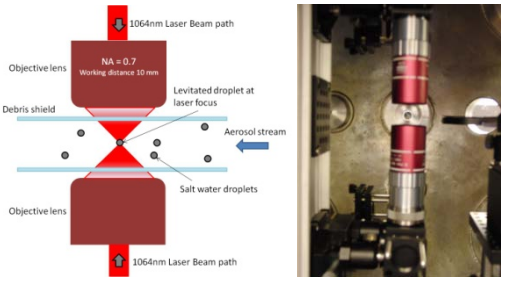

Figure 2: (left) Schematic diagram of the opposed focussed laser beams for optical levitation. (right) The centre point of the chamber is used to align the reference trapping position. The interaction laser enters through the port shown to the rear of the chamber.

For the optical trapping apparatus separate laser beams were required for each of the counter-propagating pathways. Therefore, two optical fibers' were used to couple the laser into the optical path of the objective lenses. The use of fiber optic delivery was advantageous in enabling each of the counter-propagating pathways to be moved independently without re-alignment. The lower objective lens was mounted on an x,y,z stage to permit accurate alignment (to 1 micron). The laser power ratios were balanced using a combination of a neutral density wheel and the overall laser power. A steering mirror mounted in a conjugate focal plane to the back aperture of the objective lenses was used to adjust the laser focus positions and to create optimal trapping alignment. The trapped target and laser focus positions were imaged at x100 magnification to observe droplet stability (Figure 3).

Vacuum Chamber Modifications

The optical arrangement described above was constructed inside the vacuum chamber located in Laboratory 5A, R1 (see Figure 3). Several modifications were required to implement this set-up. The fiber optic cables were passed through the chamber walls using vacuum feed-through ports. The optical images were relayed by lenses through a chamber window to two CCD cameras external to the chamber and a motorized x,y,z stage was computer controlled from outside the chamber.

Experimental

In these initial experiments nebulised droplets of salt water, 1 to 5 microns diameter, were delivered in a flow stream to the trapping region whilst the chamber was open. A single droplet was trapped and the chamber was then carefully sealed and

evacuated. The evacuation was performed using a scroll pump which was pumping on a closed valve at the time of trapping. The valve was then carefully opened to start the evacuation. The procedure was used to prevent large vibrations, that occurred during the first few strokes of the pump when starting from cold, dislodging the droplet from the optical trap.

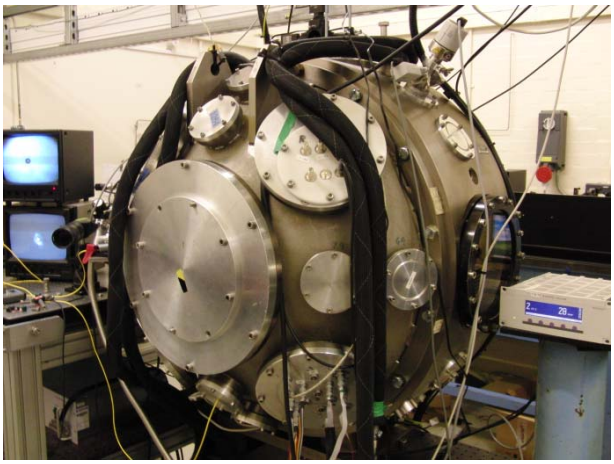

Figure 3: The vacuum chamber and diagnostics in operation. Droplet stability, laser alignment and chamber pressure are continually monitored. Trapping can be achieved from 1000 mbar to 5 mbar before efflorescence of the salt droplet occurs (i.e. a crystal is formed). The droplet is observed to be stable in position to approximately 1 micron.

As the pressure was reduced the position of the laser focus and the droplet were continually monitored (Figure 4). It was observed that the focal depth of the laser from the objective lens decreased by 52 microns as the pressure was reduced to below 20 mbar. The change was corrected using the motorized stage by decreasing the separation between the objective lenses. The droplet could be held at pressures of 9 mbar with a sodium chloride solution droplet and 5 mbar with a lithium chloride solution droplet. Beyond these pressures the droplet effloresced to a solid particle and was lost.

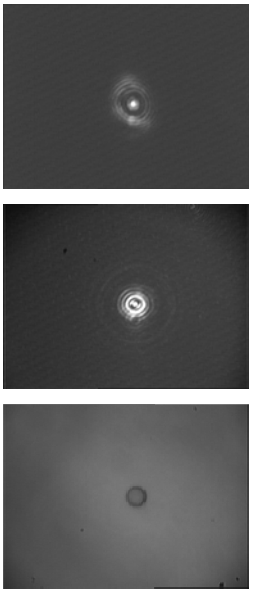

Figure 4: Images of; a) the laser focus from the lower objective, b) the laser focus from the top objective, and c) the levitated droplet. The droplet is 4 microns diameter and images are relayed from the top objective lens to a CCD camera.

Loading the trap was found to be robust and particles took less than a second to stabilise. There were no adverse effects experienced from pump vibration after the precautions outlined above. In addition, by gradual reduction of the chamber pressure no problems were experienced from air flows dislodging the droplet from the trap. From analysis of the images the target was maintained in position to within 1 micron during evacuation of the chamber.

Future Work

The next steps for extending this technology is to deliver solid particles and targets to the trapping region under vacuum conditions and to irradiate the target with a high power laser source to produce an ion beam. Solid targets will allow trapping at a higher vacuum and we plan to release micron-size particulates from dry surfaces using piezo-driven standing waves or to directly inject aerosolised solid particles.

Conclusions

We have successfully held a microscopic liquid droplet in the centre of a vacuum interaction chamber at 5 mbar using focused laser light to levitate the droplet. The droplet was held to a precision of 1 micron. By extension of this technology we aim to hold solid targets for the purpose of generating ion-beams under the LIBRA programme.

Acknowledgements

We would like to acknowledge EPSRC for funding the Basic Technology Grant (EP/E035728/1) and the STFC for access to the Lasers for Science Facility under programme access grant LSFP910.

References

1. D. Neely et al., Applied Physics Letters 89, 021502 (2006)
2. Thurn, R. and Keifer, W. Applied Optics 1985, 24, 1515G.
3. Ashkin A and Dzeidzic JM, Optical Levitation by Radiation Pressure Applied Physic Letters, 19 (8) 1971
4. Roosen and C. Imbert, Optical Levitation By Means Of Two Horizontal Laser Beams: A Theoretical And Experimental Study, Physics Letters 59A (1), 1976, 7